Kinetic Studies of DNA Cleavage Reactions Catalyzed by an ATP-Dependent Deoxyribonuclease on a 27-MHz Quartz-Crystal Microbalance†

Hisao Matsuno, Hiroyuki Furusawa, and Yoshio Okahata*

Department of Biomolecular Engineering, Frontier Collaborative Research Center, Tokyo Institute of Technology and CREST, Japan Science and Technology Corporation (JST), 4259 Nagatsuta, Midori-ku, Yokohama 226-8501, Japan

Received July 16, 2004; Revised Manuscript Received October 10, 2004

ABSTRACT: Catalytic DNA cleavage reactions by an ATP-dependent deoxyribonuclease (DNase) from *Micrococcus luteus* were monitored directly with a DNA-immobilized 27-MHz quartz-crystal microbalance (QCM). The 27-MHz QCM is a very sensitive mass-measuring device in aqueous solution, as the frequency decreases linearly with increasing mass on the electrode at a nanogram level. Three steps in ATP-dependent DNA hydrolysis reactions, including (1) binding of DNase to the end of double-stranded DNA (dsDNA) on the QCM electrode (mass increase), (2) degradation of one strand of dsDNA in the 3′ → 5′ direction depending on ATP (mass decrease), and (3) release of the enzyme from the nonhydrolyzed 5′-free-ssDNA (mass decrease), could be monitored stepwise from the time dependencies of QCM frequency changes. Kinetic parameters for each step were obtained as follows. The binding constant (K_a) of DNase to the dsDNA was determined as $(28 \pm 2) \times 10^6$ M^{-1} ($k_{on} = (8.0 \pm 0.3) \times 10^3$ M^{-1} s^{-1} and $k_{off} = (0.29 \pm 0.01) \times 10^{-3}$ s^{-1}), and it decreased to $(0.79 \pm 0.16) \times 10^6$ M^{-1} ($k'_{on} = (2.3 \pm 0.2) \times 10^3$ M^{-1} s^{-1} and $k'_{off} = (2.9 \pm 0.1) \times 10^{-3}$ s^{-1}) for the completely nonhydrolyzed 5′-free ssDNA. This is the reason the DNase bound to the dsDNA substrate can easily release from the nonhydrolyzed 5′-free-ssDNA after the complete hydrolysis of the 3′ → 5′ direction of the complementary ssDNA. K_a values depended on the DNA structures on the QCM, and the order of these values was as follows: the dsDNA having a 4-base-mismatched base-pair end (**3**) > the dsDNA having a 5′ 15-base overhanging end (**2**) > the dsDNA having a blunt end (**1**) > the ssDNA having a 3′-free end (**4**) ≫ the ssDNA having a 5′-free end (**5**). Thus, DNase hardly recognized the free 5′ end of ssDNA. Michaelis−Menten parameters (K_m for ATP and k_{cat}) of the hydrolysis process also could be obtained, and the order of k_{cat}/K_m was as follows: the dsDNA having a blunt end (**1**) ∼ the dsDNA having a 4-base-mismatched base-pair end (**3**) > the ssDNA having a free 3′ end (**4**) ≫ the ssDNA having a free 5′ end (**5**). Thus, DNase could not recognize and not hydrolyze the free 5′ end of ssDNA. The DNA hydrolysis reaction could be driven by dATP and GTP (purine base) as well as ATP, whereas the cleavage efficiency was very low driven with UTP, CTP (pyrimidine base), ADP, and AMP.

Replication is one of the key reactions in the cellular processes. In this process, many kinds of proteins including enzymes interact with nucleic acids and express various functions (*1*). An ATP-dependent deoxyribonuclease (DNase) is one of the key enzymes that hydrolyze a phosphodiester linkage between deoxyribonucleosides in the presence of ATP, and these enzymes are widely distributed in bacteria and thought to be involved in the processes of genetic recombination and recombinatorial repair of radiation damage (*2*, *3*). The ATP-dependent DNase from *Micrococcus luteus* (Mw 160 kDa) shows the activity for single- or double-stranded linear DNAs via an end-attachment 3′ → 5′ exonucleolytic procession mechanism and shows no activity for circular DNAs (*4*−*6*). So it has been used as a tool for DNA manipulation to prepare circular DNAs in vitro (*7*). The reaction mechanism of a DNA hydrolysis by this enzyme has been studied mainly in the bulk solution by measuring the accumulation of the acid-soluble hydrolysis products from radioisotope-labeled substrates as a function of time (*8*). The Michaelis−Menten constant (K_m for DNAs) and catalytic rate constant (k_{cat}) have been obtained; however, kinetic properties of the enzyme binding to the substrate DNA have not yet been characterized. And despite several improvements, this technique still has some difficulties, such as requirements of radioisotope labeling as probes and of special techniques. Gaining insights into the total enzyme reaction mechanism, it is more useful to monitor in situ all of reaction steps such as the enzyme binding, the hydrolysis along the DNA strand, and the release of the enzyme from the nonhydrolyzed DNA on the same device.

In our preliminary paper, we reported that a 27-MHz quartz-crystal microbalance (QCM)[1] is a useful tool to

† This work was partially supported by CREST, Japan Science and Technology Corporation (JST), and Research Fellowships of the Japan Society for Promotion of Science for Young Scientists.

* Corresponding author. Telephone: +81-45-924-5781. Fax: +81-45-924-5836. E-mail: yokahata@bio.titech.ac.jp.

[1] Abbreviations: QCM, quartz-crystal microbalance; NTP, nucleoside 5′-triphosphate; ATP, adenosine 5′-triphosphate; CTP, cytosine 5′-triphosphate; GTP, guanosine 5′-triphosphate; UTP, uridine 5′-triphosphate; ADP, adenosine 5′-diphosphate; AMP, adenosine 5′-monophosphate; dATP, deoxyadenosine 5′-triphosphate; ATP-γS, adenosine 5′-*O*-(3-thiotriphosphate); ATP-DNase, ATP-dependent deoxyribonuclease; NHS, *N*-hydroxysuccinimide; EDC, 1-ethyl-3-(3-dimethylaminopropyl)carbodiimide hydrochloride; P_i, inorganic orthophosphate.

10.1021/bi048486+ CCC: $30.25 © 2005 American Chemical Society
Published on Web 01/27/2005

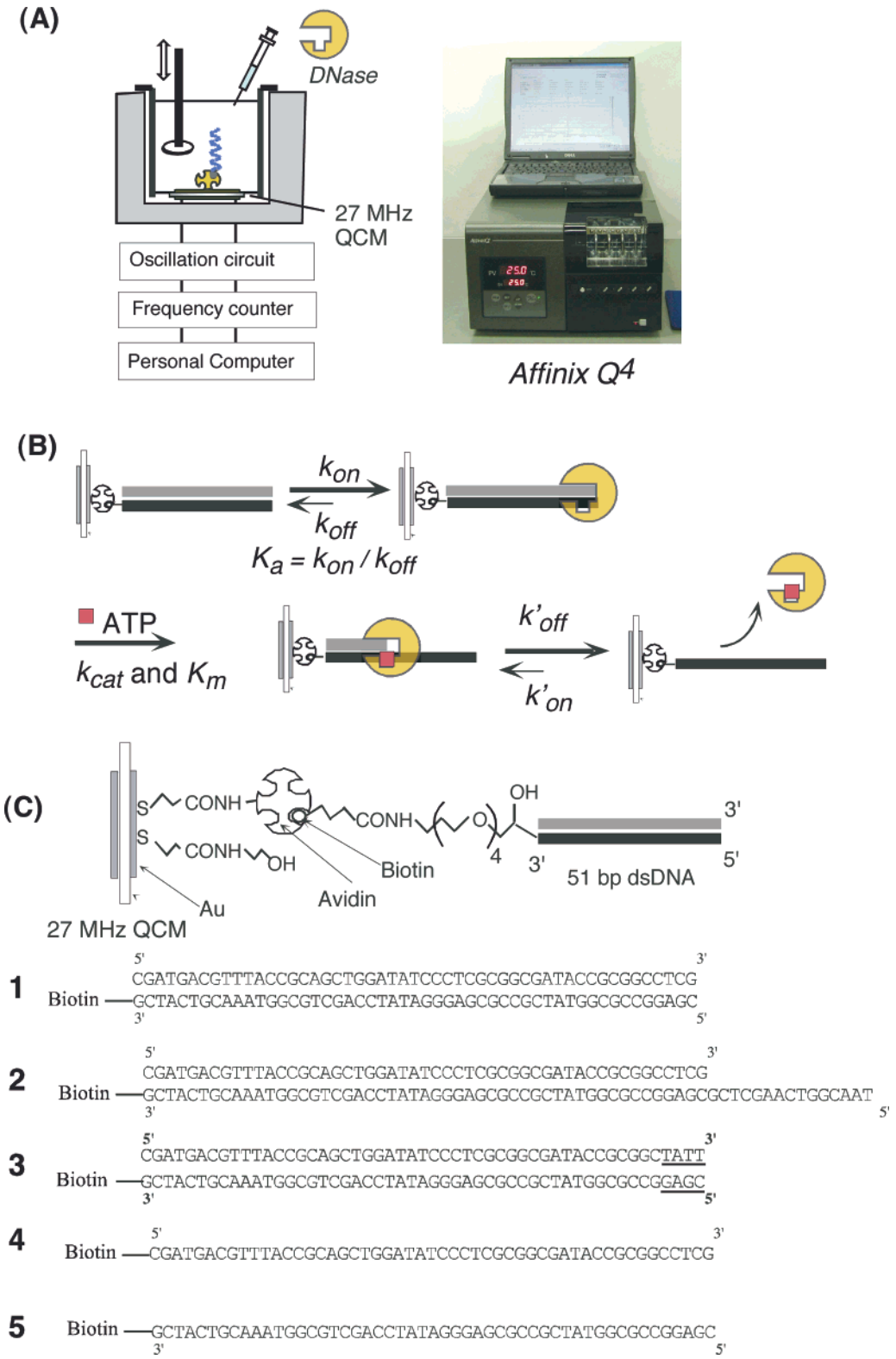

FIGURE 1: (A) Experimental setup (Affinix Q^4) for ATP-dependent hydrolyses of on a DNA-immobilized 27-MHz quartz-crystal microbalance (QCM) in buffer solution, (B) reaction schemes and kinetic parameters obtained in this work, and (C) DNA structures immobilized on an avidin-QCM.

directly detect and quantitatively analyze each step of DNA cleavage reactions in aqueous solution (see Figure 1B) (*9*). QCMs are very sensitive mass-measuring devices in aqueous solution, as well as in air, and their resonance frequency has been proved to decrease linearly with increasing mass on the QCM electrode at a nanogram level (*10*−*12*). QCM has been employed recently for investigating various biomolecular interactions on DNA strands, such as DNA hybridization (*13*), DNA−protein interactions (*14*), and DNA polymerase reactions (*15*).

In this paper, we report precise kinetic parameters of three steps in ATP-dependent DNA cleavage reactions, including (1) binding of DNase to the end of double-stranded DNA (dsDNA) on the QCM electrode (mass increase), (2)

degradation of one strand of dsDNA in the 3′ → 5′ direction depending on ATP (mass decrease), and (3) release of the enzyme from the nonhydrolyzed 5′-free-ssDNA (mass decrease) (see Figure 1B). These parameters were obtained under various conditions: (1) effect of end structures of DNA substrates such as the dsDNA having a blunt end (**1**), the dsDNA having a 5′ 15-base overhanging end (**2**), the dsDNA having a 4-base-mismatched base-pair end (**3**), the ssDNA having a free 3′ end (**4**), and the ssDNA having a free 5′ end (**5**) (see Figure 1C), and (2) effect of nucleotides on the activation of DNase (ATP, GTP, UTP, CTP, dATP, ADP, and AMP). In the binding process of DNase to DNAs, the maximum binding amount (Δm_{max}), the binding (k_{on}) and dissociation (k_{off}) rate constants, and binding constants (K_a) were obtained. In the following cleavage step, the catalytic hydrolysis rate constant (k_{cat}) and Michaelis constant (K_m for nucleotides) for enzyme reactions could be obtained. In the release process of DNase from the nonhydrolyzed ssDNA, the dissociation (k'_{off}) and rebinding (k'_{on}) rate constants, and binding constants (K'_a) were obtained. The 27-MHz QCM used in this study has a sensitivity of 0.62 ng cm^{-2} of mass change per 1 Hz of frequency decrease (*9*, *12*−*16*). This sensitivity is sufficiently large to sense the binding of enzyme and the DNA cleavage process.

EXPERIMENTAL PROCEDURES

Materials. DNase from *Micrococcus luteus* was purchased from TOYOBO (Tokyo, Japan). Each NTP was purchased from Amersham Biosciences (Tokyo, Japan). Oligonucleotides were purchased from Sawady Technology (Tokyo, Japan). dATP was purchased from TaKaRa (Shiga, Japan). ADP, AMP, and ATP-γS were from SIGMA-Aldrich (Tokyo, Japan). All other reagents were purchased from Nacalitesque (Kyoto, Japan) and used without further purification.

The 27-MHz QCM System and Its Calibration in Aqueous Solution. An *AffinixQ*[4] was used as a QCM instrument (Initium Co. Ltd, Tokyo, http://www.initium 2000.com) having four 500 μL cells equipped with a 27 MHz QCM plate (8 mm diameter of a quartz plate and an area of 4.9 mm^2 of Au electrode) at the bottom of the cell and the stirring bar with the temperature controlling system (*16*). Sauerbrey's equation (*10*) was obtained for the AT-cut shear mode QCM in the air phase,

$$\Delta F = -\frac{2F_0^{\,2}}{A\sqrt{\rho_q \mu_q}}\Delta m \qquad (1)$$

where ΔF is the measured frequency change [Hz], F_0 is the fundamental frequency of the quartz crystal prior to a mass change [27×10^6 Hz], Δm is the mass change [g], A is the electrode area [0.049 cm^2], ρ_q is the density of quartz [2.65 g cm^{-3}], and μ_q is the shear modulus of quartz [2.95×10^{11} dyn cm^{-2}]. In the air phase, 0.62 ng cm^{-2} of mass increase per 1 Hz of frequency decrease is expected. However, when the QCM is employed in an aqueous solution, we should consider effects of interfacial liquid properties (*i*.e. density, viscosity, and elasticity), thin film viscoelasticity on the QCM (*17.18*), electrode morphology (*19*), and mechanism of acoustic coupling impacts on the QCM oscillation behavior (*20*). We therefore directly calibrated the relation between ΔF and Δm by changing the immobilized amount of proteins (avidin) and biotinylated DNAs on the Au electrode of the 27-MHz QCM (*14*).

To the cleaned bare Au electrode was immobilized 3,3′-dithiodipropionic acid, and then carboxylic acids were activated as N-hydroxysuccimide esters on the surface. The activated carboxyl groups were reacted with surface amino groups of avidin (Mw. 68000). The frequency decrease reached equilibrium around 800 Hz in about 1 h (10 mM Tris-HCl, pH 7.8, 200 mM NaCl, 30 °C), and the immobilized amount of avidin was regulated by the reaction time. Avidin was not removed from the Au electrode by rinsing it with an aqueous buffer solution several times. The unreacted carboxyl groups were deactivated to hydroxyl groups by the reaction with ethanolamine (*14*). The 3′-biotinylated dsDNA (**1**) (51 bp, in Figure 1C) were injected to the avidin-immobilized QCM (10 mM Tris-HCl, pH 7.8, 200 mM NaCl, 30 °C). The frequency decrease reached equilibrium around 200 Hz in about 30 min., and the immobilized amount was regulated again by the reaction time.

The frequency changes in the solution (ΔF_{aq}) and ΔF_{air} after drying under vacuum in nitrogen for 1 h were measured at different immobilization amounts of avidin and the biotinylated DNAs, in which ΔF_{air} reflects an real mass change (Δm). There was a good linear correlation between ΔF_{aq} and ΔF_{air} with a slope of 0.98 ± 0.20. This indicates that frequency changes in the aqueous phase are nearly equal to frequency changes in the air phase when the same mass was loaded on the Au electrode. Thus, the Sauerbrey's equation (−0.62 ng cm^{-2} per 1 Hz for the 27-MHz QCM) can be applied even in the aqueous solution limited to the immobilization of a globular proteins such as avidin (Mw. 68000) and a short oligonucleotides (ca. 50 bp) (*12*−*16*). When the long dsDNA (500−1000 bp) was immobilized on the QCM, however, the slope was different between in the air and aqueous phases due to the hydration and viscoelastic long DNA strands on the QCM.

The noise level of the 27 MHz QCM was ±1 Hz in buffer solutions at 30 °C, and the standard deviation of the frequency was ±2 Hz for 2 h in buffer solutions at 30 °C.

Preparation of DNA-Immobilized QCM Plates. DNA structures used in this study is summarized in Figure 1C: 3′-biotinylated dsDNA (51 bp) having a blunt end (**1**), having a 5′ 15-base overhanging end (**2**), and having a 4-base-mismatched base region at the end (underlined) (**3**), and the 5′-biotinylated ssDNAs having a 3′-free end (**4**) and the 3′-biotinylated ssDNA having a 5′-free end (**5**). Oligonucleotide duplexes were formed by mixing biotinylated strands and its complementary strands in 10 mM Tris-HCl, pH 7.8, 200 mM NaCl, boiled for a few minutes and then cooled to room temperature over 3 h. These oligodeoxyribonucleotides were immobilized on a cleaned Au electrode of the QCM using a biotin−avidin linkage and a tetraethyleneglycol spacer according to previous papers (*14*, *15*). The immobilized amount of the dsDNA (**1**) was maintained to be 60 ± 2 ng cm^{-2} (ca. 1.9 ± 0.1 pmol cm^{-2}). This corresponds to approximately 4% coverage of the Au surface, and this small coverage would give enough space for binding of a large enzyme molecule. Immobilized amounts of other DNAs were also maintained to be 1.9 ± 0.1 pmol cm^{-2} (4% coverage).

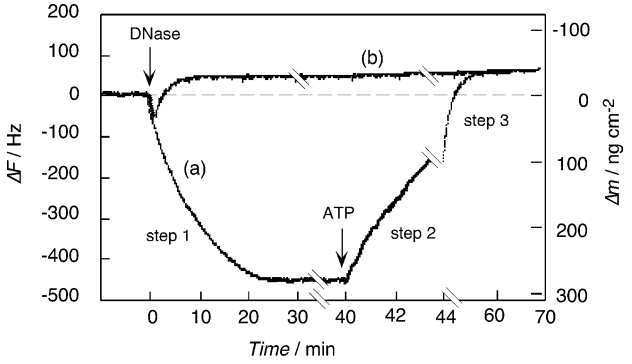

FIGURE 2: Typical time courses of frequency changes of the dsDNA (**1**)-immobilized QCM, responding to the addition of DNase and ATP. (a) DNase was added at a first arrow and then excess ATP was added at a second arrow. (b) DNase was added in the presence of excess ATP. ([DNase] = 138 nM, [ATP] = 0.5 mM, 67 mM Glyc ine-NaOH, pH 7.9, 30 mM $MgCl_2$, 8.4 mM 2-mercaptoethanol, and 0.1% Nonidet P-40, 30 °C).

Enzyme Reactions on a DNA-Immobilized QCM Cell. A DNA-immobilized QCM cell was filled with 500 μL of buffer solution containing 67 mM Glycine-NaOH, pH 7.9, 30 mM $MgCl_2$, 8.4 mM 2-mercaptoethanol, and 0.1% Nonidet P-40 and placed until the resonance frequency was kept constant (±1 Hz for 30 min). Frequency changes responding to the addition of the enzyme and/or various nucleotide solutions into the cell were followed with time. The solution was stirred to avoid any effect of diffusion of the enzyme and nucleotides, and the stirring did not affect the stability and magnitude of frequency changes.

RESULTS AND DISCUSSION

In Situ Monitoring of DNA Cleavage Reactions by an ATP-Dependent DNase. Figure 2 shows typical frequency changes of the dsDNA (**1**)-immobilized QCM cell as a function of time, responding to the addition of DNase and ATP into the aqueous solution. In curve (a), the frequency decreased (mass increased) gradually for approximately 30 min, responding to the addition of the DNase solution at the first arrow (final concentration; 138 nM), due to the slow binding of DNase to the dsDNA (**1**) (step 1). The binding amount at equiliblium was 280 ± 10 ng (1.8 ± 0.1 pmol) cm^{-2}, indicating that one DNase binds to the dsDNA by 1:1 ratio, since 1.9 ± 0.1 pmol (60 ± 2 ng) cm^{-2} of the dsDNA (**1**) was immobilized on the QCM cell. It was confirmed that DNase hardly bound to an avidin surface without DNAs (data not shown). When an excess ATP solution (final concentration 0.5 mM) was added at the second arrow of curve (a), the frequency rapidly increased (mass decreased) to the constant value (−30 ± 3 ng cm^{-2} over the starting point) within a several minutes (steps 2 and 3). This indicates that DNase bound on the substrate was activated by ATP and could hydrolyze DNA strands. As a control experiment, when γS-ATP that could be hardly hydrolyzed by DNase was added instead of ATP, no frequency changes could be observed (data not shown).

On the other hand, when ATP was present in advance and then the enzyme was injected, the frequency slightly decreased at first and then increased (mass decreased) as shown in curve (b) and reached the same mass decrease as shown in curve (a). The decreased mass from the starting point was 30 ng (1.9 ± 0.1 pmol) cm^{-2}, corresponding to 50 ± 5% of the immobilized dsDNA (**1**) (60 ± 2 ng (1.9 ± 0.1 pmol) cm^{-2}): the one strand was completely hydrolyzed. Since the ATP-dependent DNase is reported to hydrolyzes dsDNA from the 3′-end (*4*), the 3′ → 5′ hydrolysis occurs only at the upper strand of dsDNA because the 3′-end of the lower strand is blocked by a biotin−avidin linkage (see Figure 1C). Thus, the mass decrease in steps 2 and 3 of curve (a) reflects two processes: the complete 3′ → 5′ hydrolysis of the upper strand of immobilized dsDNA (**1**) and the release of the enzyme from the QCM after the hydrolysis, respectively. Frequency changes in curve (b) also reflect the mass decrease due to the hydrolysis on the QCM electrode.

In curve (b) of Figure 2, the continuous frequency decrease and increase reflect the continuous reactions of the enzyme binding, hydrolysis, and the release of the enzyme, and it maybe difficult to separate each step for analyzing kinetic parameters. Therefore, we chose the stepwise reaction of curve (a) to analyze kinetically each step: (1) binding DNase to the end of dsDNA, (2) DNA degradation of the upper strand of dsDNA in the 3′ → 5′ direction, and (3) release of the enzyme from the remaining nonhydrolyzed 5′-free ssDNA.

Binding Process of DNase on Various Ends of DNAs. The DNase binding process to DNAs (step 1 of curve (a) in Figure 2) is described by eq 2. The amount of the DNA/DNase complex formed at time t after injection is given by eqs 3−5. The relaxation time (τ) of DNase binding is

$$\mathrm{DNA} + \mathrm{DNase} \underset{k_{\mathrm{off}}}{\overset{k_{\mathrm{on}}}{\rightleftharpoons}} \mathrm{DNA/DNase} \quad (2)$$

$$[\mathrm{DNA/DNase}]_t = [\mathrm{DNA/DNase}]_!\{1 - \exp(-t/\tau)\} \quad (3)$$

$$\Delta m_t = \Delta m_!\{1 - \exp(-t/\tau)\} \quad (4)$$

$$1/\tau = k_{\mathrm{on}}[\mathrm{DNase}]_0 + k_{\mathrm{off}} \quad (5)$$

calculated from curve fitting of QCM frequency changes at various enzyme concentrations (5−400 nM). DNase binding and dissociation rate constants (k_{on} and k_{off}) could be obtained from the slope and intercept of the plot of $\tau^{-\mu}$ against DNase concentration (eq 5). The binding constants (K_a) could be also obtained from the ratio of k_{on} to k_{off}.

Figure 3A shows typical time courses for DNase binding to the dsDNA (**1**) with different DNase concentrations (13−69 nM). DNase binding amounts increase with the increase in DNase concentrations. Similar time courses with DNase concentrations (5−400 nM) were observed for other DNAs (**2**) -(**5**); the binding and dissociation rate constants (k_{on} and k_{off}) were obtained according to eq 5 (Figure 3B). The results are summarized in Table 1, together with the QCM binding amount (Δm) when DNase was injected at 35 nM.

In the case of dsDNAs (**1**, **2**, and **3**), the DNase binding amounts (Δm) were large and independent of terminus structures (70−80 ng cm^{-2}). When the injected concentrations of DNase were increased (5−400 nM), the binding amount of DNase showed the saturation behavior with the maximum binding amount (Δm_{max} = 320 ± 30 ng (1.9 ±

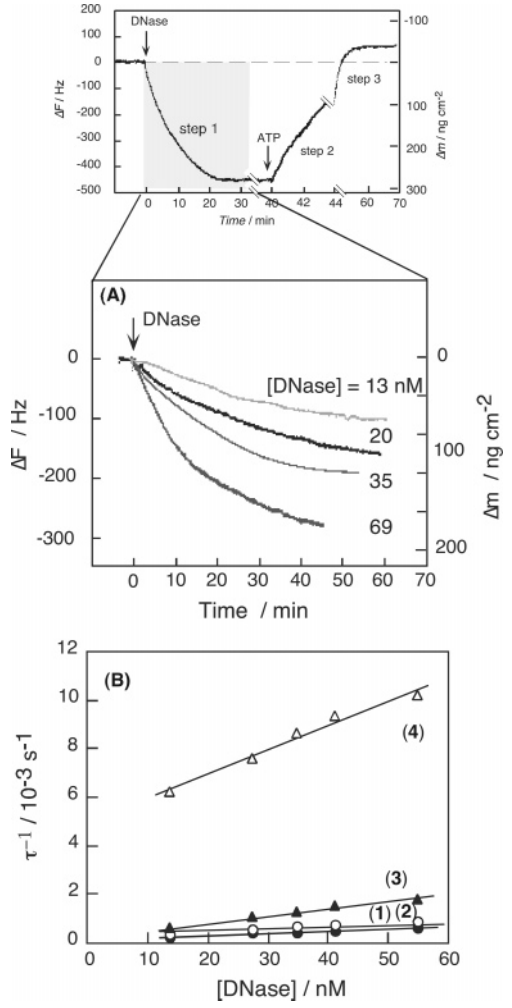

FIGURE 3: (A) Binding behaviors of DNase to the dsDNA (**1**) dependent on the DNase concentrations. ([DNase] = 13−69 nM, [dsDNA] = 60 ± 2 ng (1.9 pmol) cm^{-2} on the QCM, 67 mM Glycine-NaOH, pH 7.9, 30 mM $MgCl_2$, 8.4 mM 2-mercaptoethanol, and 0.1% Nonidet P-40, 30 °C). (B) Linear reciprocal plots of relaxation time (τ) against DNase concentration according to eq 5. (●) the dsDNA having a blunt end (**1**), (○) the dsDNA having 5′ 15-base overhanging end (**2**), (▲) the dsDNA having a 4-base mismatched base-pair end (**3**), and (△) the ssDNA having a 3′-free end (**4**).

Table 1: Binding Amount (Δm), Binding and Dissociation Rate Constants (k_{on} and k_{off}), and Binding Constants (K_a) of DNase for Various DNAs[a]

DNA[b]	Δm^c / ng (pmol) cm^{-2}	$k_{on}{}^d$ / 10^3 M^{-1} s^{-1}	$k_{off}{}^d$ / 10^{-3} s^{-1}	$K_a{}^e$ / 10^6 M^{-1}
1	72 ± 6 (0.42 ± 0.04)	8.0 ± 0.3	0.29 ± 0.01	28 ± 2
		$k'_{on}{}^f$=2.3 ± 0.2	$k'_{off}{}^f$=2.9 ± 0.1	$K'_a{}^f$=0.79 ± 0.16
2	80 ± 5 (0.47 ± 0.03)	7.9 ± 0.1	0.14 ± 0.01	56 ± 6
3	81 ± 6 (0.48 ± 0.03)	28 ± 4	0.19 ± 0.02	140 ± 50
4	25 ± 5 (0.15 ± 0.02)	97 ± 7	4.9 ± 0.5	19 ± 5
5	< 1 (< 0.01)	0.91 ± 0.21	5.3 ± 1.1	0.17 ± 0.09

[a] Binding experiments were carried out at different DNase concentrations (5−400 nM) depending on DNA sequences. [b] Sequences are shown in Figure 1C. [c] Binding amount at [DNase] = 35 nM. [d] Obtained from eqs 3−5 in the text. [e] Ratio of k_{on} to k_{off}. [f] Obtained from eqs 10−12 in step 3.

0.2 pmol) cm^{-2}) for dsDNAs (**1**,**2**, and **3**). Since dsDNAs were immobilized in the range of 60 ± 5 ng (1.9 ± 0.2 pmol) cm^{-2}) on the QCM, DNase can bind to dsDNAs by a 1:1 ratio. Dorp and co-workers reported that the formation of 2:1 complexes of DNase with a linear dsDNA in the bulk buffer solution was identified by a density-gradient centrifugation method and suggested the enzyme bound to two free ends of dsDNA *(5)*. The 1:1 binding of DNase to dsDNA is reasonable in our system, because the one end is blocked by biotin−avidin linkage on the QCM plate. The binding amount of DNase to the ssDNA having a 3′-free hydroxyl end (**4**) was largely decreased (Δm = 25 ± 5 ng cm^{-2}) and DNase hardly bound to the ssDNA with a 5′-free hydroxyl end (**5**).

The binding constant of the dsDNA having the 5′-free overhanging end (**2**) (K_a = (56 ± 6) × 10^6 M^{-1}) was 2 times larger than that of the dsDNA with the blunt end (**1**) ((28 ± 2) × 10^6 M^{-1}) due to the decreasing k_{off} values from (0.29 ± 0.01) × 10^{-3} s^{-1} to (0.14 ± 0.01) × 10^{-3} s^{-1}. Since the structure of the dsDNA (**2**) is similar to that of on the way of the hydrolysis, this is reasonable for the enzyme to suppress the dissociation from the DNA substrate to enhance the processivity of the hydrolysis. The k_{off} values for the ssDNA both of (**4**) and (**5**) were almost same ((4.9−5.3) × 10^{-3} s^{-1}) but the k_{on} value for the 3′-free ssDNA (**4**) ((97 ± 7) × 10^3 M^{-1} s^{-1}) was extreme large compared to that for the 5′-free ssDNA (**5**) ((0.91 ± 0.21) × 10^3 M^{-1} s^{-1}), and DNase hardly bound to the 5′ free DNA (**5**) due to the very small K_a value ((0.17 ± 0.09) × 10^6 M^{-1}). These results indicate that DNase can bind to the 3′-end, but hardly to the 5′-end and can remain more easily on the dsDNA than the ssDNA. This is very reasonable to consider the hydrolysis direction of this enzyme (3′ → 5′). The largest K_a value of (140 ± 50) × 10^6 M^{-1} was obtained for the 4-base mismatched dsDNA (**3**) due to both of the large k_{on} and small k_{off} values. This result was contributed from easy recognition at the 3′-free end of the melting and mismatched bases and slow dissociation from the double-stranded structure. The Klenow fragment of DNA polymerase I from *Escherichia coli* consists of a 5′ → 3′ polymerase unit and also a 3′ → 5′ exonuclease unit. It is known that the primer/template region containing mismatched bases or many AT base pairs is preferentially recognized by the exonuclease unit of the enzyme but hardly recognized by the polymerase unit (*21*). Considering the necessity of the melting end of the dsDNA substrate to hydrolyze DNA molecules, it is general that the exonuclease could easily recognize the melting end of the dsDNA.

Effect of Enzyme Concentrations on the DNA Cleavage Process. Figure 4A shows the entire reaction process when DNase was added at the first arrow at different concentrations (20, 35, and 69 nM in solution) and then excess ATP was added at the second arrow using the dsDNA (**1**)-immobilized QCM. Final frequency changes at the steady state were the same (−30 ng cm^{-2}) independent of DNase concentrations. Figure 4B shows the reaction process when ATP was added at different times prior to binding equilibration for DNase (135 nM added in the solution). In these cases, the cleaved amounts were also ca. 30 ng cm^{-2} independent of the time of the ATP additions, and these results indicate that DNA cleavage was completed. The amount of DNase bound on dsDNA and the initial rate (v_o) of DNA cleavage just after enzyme injection were calculated from the QCM mass increases observed after enzyme injection and the slope of

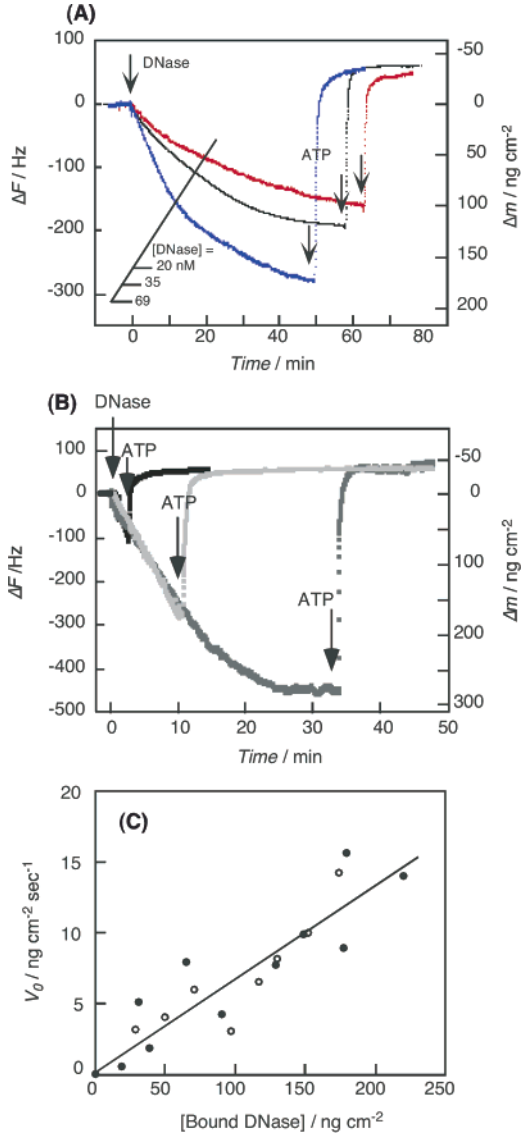

FIGURE 4: Cleavage processes dependent on (A) the DNase concentration in the bulk solution (20, 35, and 69 nM), in which ATP added after the equilibrium of the DNase binding. and (B) the DNase concentration bound on the dsDNA (**1**) end, in which ATP added before the equilibrium of the DNase binding. (67 mM Glycine-NaOH, pH 7.9, 30 mM $MgCl_2$, 8.4 mM 2-mercaptoethanol, and 0.1% Nonidet P-40, 30 °C). (C) Plot of initial hydrolysis rates (v_0) just after the ATP injections against the concentrations of the bound DNase on the dsDNA (**1**) obtained from (●) the mass increase after the DNase injection in (A) and (○) the mass increase after the DNase injection of (B).

QCM mass decrease observed just after ATP injection in Figures 4A and 4B, respectively. The v_o values were plotted against the concentration of bound DNase (Figure 4C). The DNA cleave rate increased linearly with the bound amount of DNase on the DNA (**1**). These results clearly indicate that the enzyme catalyzing the cleavage is the bound DNase on the DNA, but not the enzyme in bulk solution.

Michaelis−Menten Kinetics of DNA Cleavage Process. DNA cleavage reactions (step 2 of curve (a) of Figure 2) were initiated by the addition of ATP after the formation of the DNA/DNase complex on the QCM. The cleavage process is expressed simply by the Michaelis−Menten reaction between the DNA/DNase complex and added ATP as shown in eqs 6−8, where DNA′ indicates shortened DNA and DNA″ indicates released nucleotide products with degradation.

Table 2: Michaelis Constant of ATP (K_m) and Catalytic Cleaved Rate Constant (k_{cat}) in the DNA/DNase Complex on the QCM[a]

DNA[b]	k_{cat} / 10^3 s^{-1}	K_m / 10^{-6} M	k_{cat} / K_m 10^6 $M^{-1}s^{-1}$
1 3′ 5′	4.0 ± 0.1	15 ± 1	270 ± 30
3 3′ 5′	3.9 ± 0.2	14 ± 1	280 ± 35
4 3′	0.7 ± 0.1	11 ± 1	64 ± 15
5 5′	nd[c]	nd[c]	nd[c]

[a] [DNA/DNase complex] = 1.7 pmol cm^{-2} in the solution. [b] Sequences are shown in Figure 1C. [c] Could not be detected.

$$\text{DNA/DNase} + \text{ATP} \overset{K_m}{\rightleftharpoons} \text{DNA/DNase/ATP} \xrightarrow{k_{cat}} \text{DNA}'\text{/DNase} + \text{DNA}'' + \text{ADP} + \text{P}_i \quad (6)$$

$$V_0 = \frac{k_{cat}[\text{DNA/DNase}][\text{ATP}]_0}{K_m + [\text{AT}]_0} \quad (7)$$

$$\frac{1}{V_0} = \frac{K_m}{k_{cat}[\text{DNA/DNase}]} \rightleftarrows \frac{1}{[\text{ATP}]_0} + \frac{1}{k_{cat}[\text{DNA/DNase}]} \quad (8)$$

The QCM resonance frequency was defined as the zero position at the point of addition of ATP solution; the frequency changes were then recorded with time. When the initial concentration of DNA/DNase was fixed at 1.7 pmol cm^{-2} on the QCM, the hydrolysis processes occurred after the injection of various concentrations of ATP in the solution (Figure 5A). The initial hydrolysis rate (v_0) increased with the addition of ATP, and Figure 5B shows the plot of v_0 against ATP concentrations. From the reciprocal plot inserted in Figure 5B, Michaelis constants of ATP (K_m), cleavage catalytic rate constants (k_{cat}), and apparent second-order rate constants (k_{cat}/K_m) were obtained from the slope and intercept of eq 8. The results for the dsDNA (**1**) are summarized in Table 2, together with those obtained for various DNAs on the QCM.

The K_m for ATP was independent of DNA structures, indicating the ATP recognition site in DNase was unaffected by the DNA recognition. The K_m value of 15 ± 1 μM for ATP obtained in this work was consistent with those values (50 μM) obtained in the bulk solution of the similar types of DNase (*8*). The catalytic efficiency was the same between the dsDNA with a blunt end (**1**) and a mismatched end (**3**) with the similar k_{cat} and K_m values. It is interesting that the 4-base mismatch at the end of dsDNA only affected the enzyme binding process but not the hydrolysis process. DNase can hydrolyze from the 3′end of both ssDNA and dsDNA, but the catalytic efficiency for the ssDNA (**4**) (k_{cat} = (0.7 ± 0.1) × 10^3 s^{-1}) was largely decreased in comparison with those of dsDNAs (**1** and **3**) (k_{cat} = (3.9 ± 0.1) × 10^3 s^{-1} and (4.0 ± 0.1) × 10^3 s^{-1}, respectively). Although it is difficult to explain why k_{cat} value for the

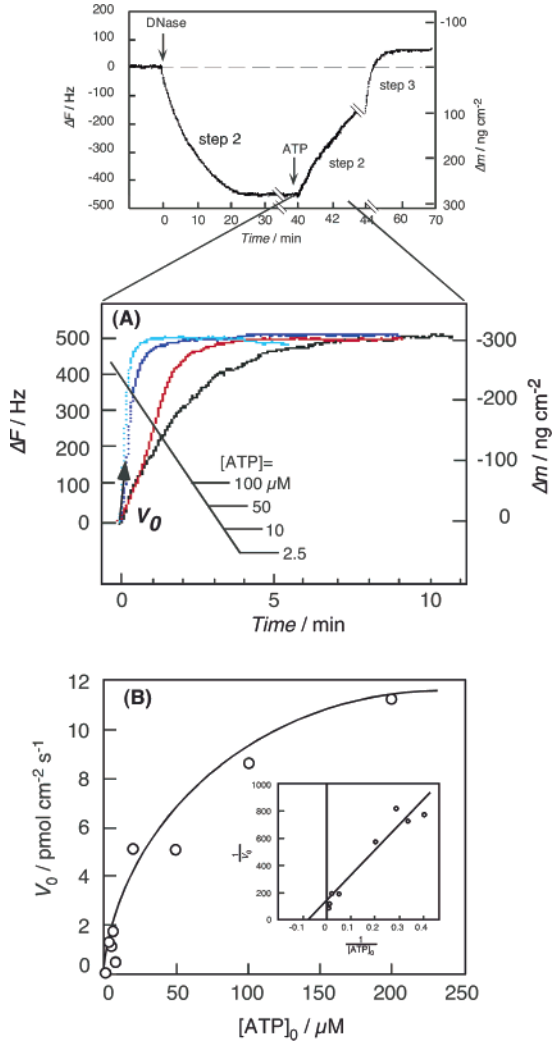

FIGURE 5: (A) Time courses of the hydrolysis process on the dsDNA (**1**)-immobilized QCM electrode, depending on ATP concentrations (2.5−100 μM). (B) Saturation behavior of initial elongation rates (v_0) against ATP concentrations. Lineweaver−Burk plot according to eq 8 was inserted. ([DNA/DNase]$_0$ = 1.7 pmol cm^{-2}, 67 mM Glycine-NaOH, pH 7.9, 30 mM MgCl2, 8.4 mM 2-mercaptoethanol, and 0.1% Nonidet P-40, 30 °C.).

Table 3: Michaelis Constant of Various Nucleotides (K_m) and Catalytic Cleaved Rate Constant (k_{Cat}) in the DNA/DNase Complex on the DsDNA (**1**)-Immobilized QCM Plate[a]

nucleotide	$k_{cat}/10^3$ s^{-1}	$K_m/10^{-6}$ M	$(k_{cat}/K_m)/10^6$ M^{-1} s^{-1}
ATP	4.0 ± 0.1	15 ± 1	270 ± 30
dATP	3.6 ± 0.3	14 ± 2	260 ± 60
GTP	1.9 ± 0.1	76 ± 14	26 ± 7
UTP	1.7 ± 0.2	270 ± 22	6.3 ± 2.4
CTP	1.8 ± 0.1	220 ± 15	8.1 ± 1.2
ADP	2.1 ± 0.4	150 ± 10	14 ± 4
AMP	*b*	*b*	*b*

[a] [DNA/DNase complex] = 1.7 pmol cm^{-2} in the solution. [b] Could not be detected.

ssDNA is smaller than those for dsDNA, it is reasonable to consider that DNase shows smaller K_a value for the ssDNA than the dsDNA and the k_{cat} for the ssDNA will decrease.

Effect of Various Nucleotides on DNA Cleaved Process. Recognition ability of DNase for other types of nucleotides was investigated. Table 3 shows K_m values for various nucleotides, cleaved rate constants, k_{cat}, and the apparent second-order rate constants (k_{cat}/K_m) for the dsDNA (**1**).

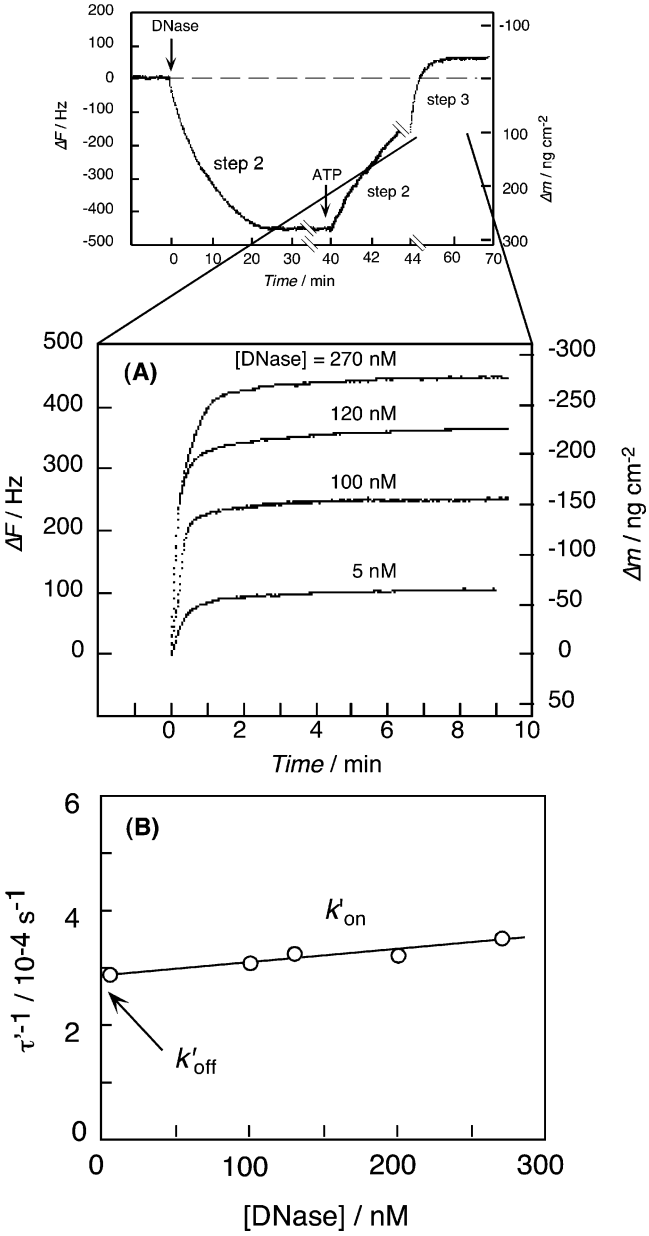

FIGURE 6: (A) Release behavior of DNase from the completely hydrolyzed DNA depending on the bound amount of DNase on the dsDNA (**1**). (B) Linear reciprocal plot of relaxation time (τ') against DNase concentrations according to eq 12. (67 mM Glycine-NaOH, pH 7.9, 30 mM $MgCl_2$, 8.4 mM 2-mercaptoethanol, and 0.1% Nonidet P-40, 30 °C).

DNase can recognize dATP as well as ATP with the similar K_m value. The binding ability (K_m) of DNase for nucleotides decreased for pyrimidine bases (UTP and CTP) compared with purine bases such as adenine and with decreasing phosphate groups in nucleotides. Thus, DNase strictly recognizes both a purine base and a triphophate bone but not tightly the 2′-hydroxy group of a ribose.

DNase Dissociation Process. DNase dissociation from the productive ssDNA (step 3 of curve (a) of Figure 2) was observed as quick frequency increases (mass decreases) on the QCM following the DNA cleavage process. The resonance frequency of the QCM was defined as the zero position at the time of cleavage completion (−30 ng cm^{-2} from the point of addition of ATP solution), and the frequency increase was recorded with time. In Figure 6A, the enzyme

dissociation process was monitored at different DNase concentrations using the dsDNA (**1**) on the QCM.

The dissociation process is described by eq 9. The amount of DNA/DNase complex left at time t is given by eqs 10−12.

$$\mathrm{DNA'} + \mathrm{DNase} \underset{k'_{off}}{\overset{k'_{on}}{\rightleftharpoons}} \mathrm{DNA'/DNase} \quad (9)$$

$$-[\mathrm{DNA'/DNase}]_t = -[\mathrm{DNA'/DNase}]_! \{1 - \exp(-t/\tau')\} \quad (10)$$

$$-\Delta m_t = -\Delta m_! \{1 - \exp(-t/\tau')\} \quad (11)$$

$$1/\tau' = k'_{on}[\mathrm{DNase}]_0 + k'_{off} \quad (12)$$

The dissociation and rebinding rate constants (k'_{off} and k'_{on}) and binding constants (K'_a) for the dissociation process could be obtained similarly to that for step 1, and the results are summarized in the second line of Table 1. The rebinding rate constant ($k'_{on} = (2.3 \pm 0.2) \times 10^3\ M^{-1}\ s^{-1}$) in step 3 was one-fourth compared to the binding rate constant ($k_{on} = (8.0 \pm 0.3) \times 10^3\ M^{-1}\ s^{-1}$) in step 1. On the contrary, the dissociation rate constant ($k'_{off} = (2.9 \pm 0.1) \times 10^{-3}\ s^{-1}$) in step 3 was 10 times larger than the dissociation rate constants ($k_{off} = (0.29 \pm 0.01) \times 10^{-3}\ s^{-1}$) in step 1. As a result, the binding constant ($K'_a = (0.79 \pm 0.16) \times 10^6\ M^{-1}$) of DNase to the reminded nonhydrolyzed DNA (i.e. 5′-free ssDNA) in step 3 was 35 times smaller than $K_a = (28 \pm 2) \times 10^6\ M^{-1}$ for the prehydrolyzed dsDNA (**1**) in step 1. Since the remained DNA structure after the hydrolysis is similar to the ssDNA with a 5′-free end (**5**), k'_{on} and k'_{off} values were obtained as similar values of k_{on} and k_{off} values for the ssDNA with a 5′-free end in step 1. Thus, DNase has a stronger binding ability to the starting dsDNA than to the hydrolyzed ssDNA with a 5′-free end, and DNase can release from the completely hydrolyzed terminus as shown in curve (a) of Figures 2 due to both the slow rebinding rate and the fast releasing rate.

CONCLUSION

We have determined all kinetic parameters for a three-step DNA cleavage reaction by ATP-dependent DNase from *Micrococcus luteus* using a DNA-immobilized 27-MHz QCM: DNase binding of the dsDNA (**1**) with $K_a = 10^7\ M^{-1}$ ($k_{on} = 10^3\ M^{-1}\ s^{-1}$ and $k_{off} = 10^{-4}\ s^{-1}$), depending on the terminus structure of DNAs (step 1). Michaelis−Menten parameters of DNase in the hydrolysis process ($K_m = 10^{-5}$ M for ATP, $k_{cat} = 10^3\ s^{-1}$, and $k_{cat}/K_m = 10^8\ M^{-1}\ s^{-1}$), depending on nucleotides structures (step 2), and DNase can easily release from the hydrolyzed strand with $K'_a = 10^6\ M^{-1}$ ($k'_{on} = 10^3\ M^{-1}\ s^{-1}$ and $k'_{off} = 10^{-3}\ s^{-1}$) (step 3). This is the first example of investigating both kinetically and quantitatively the binding, catalysis, and release processes of ATP-dependent deoxyribonuclease reactions in situ on the same device.

We believe that the 27-MHz QCM system (Affinix Q^4) is highly sensitive in the detection of in situ enzyme reactions on a DNA strand without any labeling. This system will become applicable for other DNA/RNA enzyme reactions such as ligation and restricted enzyme reactions.

REFERENCES

1. Kornberg, A., and Baker, T. (1992) *DNA Replication*, 2nd ed., Freeman, New York.
2. Hout, A., Oosterbaan, R. A., Pouwels, P. H., and de Jonge, A. J. R. (1970) Purification of an ATP-dependent nuclease from *Micrococcus lysodeikticus*, *Biochim. Biophys. Acta 204*, 632−635.
3. Anai, M., Hirahashi, T., and Takagi, Y. (1970) A Deoxyribonuclease which requires nucleoside triphosphate from *Micrococcus lysodeikticus*, *J. Biol. Chem. 245*, 767−774.
4. Cerio-Ventura, G., Fossato, M., Vellante, A., Palitti, F., Fasella, P. M., and Whitehead, E. P. (1981) ATP-dependent exonuclease V from *Micrococcus luteus*, The enzyme-DNA complex, the processive mechanism, and the role of ATP, *Biochim. Biophys. Acta 652*, 283−293.
5. Dorp, B. V., Ceulen, TH. E., Heijneker, H. L., and Pouwels, P. H. (1973) Properties of an ATP-dependent deoxyribonuclease from *Micrococcus luteus*. Evidence for a stable DNA-enzyme complex, *Biochim. Biophys. Acta 299*, 65−81.
6. Dorp, B. V., Caulen, M. TH. E., and Pouwels, P. H. (1974) Properties of an ATP-dependent deoxyribonuclease from *Micrococcus luteus*. A characterization of the reaction products, *Biochim. Biophys. Acta 340*, 166−176.
7. Yamagishi, H., Tsuda, T., Fujimoto, S., Toda, M., Kato, K., Maekawa, Y., Umeno, M., and Anai, M. (1983) Purification of small polydisperse circular DNA of eukaryotic cells by use of ATP-dependent deoxyribonuclease, *Gene 26*, 317−321.
8. Palitti, F., Vellante, A., Cerio-Ventura, G., Fasella, P., Salerno, C., and Whitehead, E. (1979) The kinetics of ATP-dependent exonuclease V from *Micrococcus lysodeikticus*. A Michaelian dependence on DNA concentration, *Eur. J. Biochem. 97*, 147−153.
9. Matsuno, H., Furusawa, H., and Okahata, Y. (2002) Direct Monitoring of DNA Cleavages catalyzed by an ATP-dependent Deoxyribonuclease on a 27 MHz Quartz-Crystal Microbalance, *Chem. Commun*. 470−471.
10. Sauerbrey, G. (1959) Use of quartz crystal vibrator for weighing thin films on a microbalance, *Z. Phys. 155*, 206−222.
11. (a) Janshoff, A., Galla, H. J., and Steinem, C., (2000) Piezoelectric Mass-Sensing Devices as Biosensors—An Alternative to Optical Biosensors?, *Angew. Chem., Int. Ed. 39*, 4004−4032. (b) Wards, M. D. Buttry, D. A. (1992) Measurement of Interfacial Processes at Electrode Surfaces with the Electrochemical Quartz Crystal Microbalance, *Chem. Rev. 92*, 1355−1379.
12. Ebara, Y., Itakura, K., and Okahata, Y. (1996) Gas Phase Selective Adsorption on Functional Monolayers immobilized on a Highly Sensitive Quartz-Crystal Microbalance, *Langmuir 12*, 5165−5170.
13. Okahata, Y., Kawase, M., Niikura, K., Ohtake, F., Furusawa, H., and Ebara, Y. (1998) Kinetic Measurements of DNA Hybridization on an Oligonucleotide-immobilized 27 MHz Quartz-Crystal Microbalance, *Anal. Chem. 70*, 1288−1296.
14. (a) Okahata, Y., Niikura, K., Sugiura, Y., Sawada, M., Morii, T. (1998) Kinetic Studies of Sequence-Specific Binding of GCN4-bZIP Peptides to DNA Stands immobilized on a 27 MHz Quartz-Crystal Microbalance, *Biochemistry 37*, 5666−5672. (b) Matsuno, H., Niikura, K., and Okahata, Y. (2001) Design and Characterization of Asparagine- and Lysine-Containing Alanine-based Helical Peptides That Bind Selectively to AT Base-Pairs of Oligonucleotides Immobilized on a 27 MHz Quartz Crystal Microbalance, *Biochemistry 40*, 3615−3622.
15. (a) Niikura, K., Matsuno, H., and Okahata, Y. (1998) Direct monitoring of DNA Polymerase Reactions on a Quartz-Crystal Microbalance, *J. Am. Chem. Soc. 120*, 8537−8538. (b) Matsuno, H., Niikura, K., and Okahata, Y. (2001) Direct Monitoring and Kinetic Studies of DNA Polymerase Reactions on a DNA-immobilized Quartz-Crystal Microbalance, *Chem. Eur. J. 7*, 3305−3312.
16. (a) Nishino, H., Nihira, T., Mori, T., and Okahata, Y. (2004) Direct Monitoring of Enzymatic Glucan Hydrolyses on a 27-MHz Quartz-Crystal Microbalance, *J. Am. Chem. Soc. 126*, 2264−2265. (b) Nishino, H., Murakawa, A., Mori, T. and Okahata, Y. (2004) Kinetic Studies of Amylopectin Cleavage Reactions Catalyzed by Phosphorylase *b* using a 27 MHz Quartz Crystal Microbalance, *J. Am. Chem. Soc., 126*, 14752−14757. (c) Nihira, T., Mizuno, M., Tonozuka, T., Sakano, T., Mori, T., and Okahata, Y., Direct Monitoring of Site-directed Mutagenic Isomalto-Dextranase catalyzed Hydrolytic Reactions on a 27 MHz Quartz-crystal Microbalance, *Angew. Chem., Int. Ed.*, submitted.
17. (a) Nomura, T., Okuhara, M. (1982) Frequency shifts of piezoelectric quartz crystals immersed in organic liquids, *Anal. Chim.*

Acta 142, 281−284. (b) Bruckenstein, S., Shay, M. (1985) Experimental aspects of use of the quartz crystal microbalance insolution, *Electrochem. Acta 30*, 1295−1300. (c) Kanagawa, K. K. Gordon, J. (1985) The oscillation frequency of a quartz resonator in contact with liquid, *Anal. Chim. Acta 175*, 99−105.

18. (a) Hook, F., Rhodahl, M., Brzezinski, P., Kasemo, B. (1998) Energy Dissipation Kinetics for Protein and Antibody−Antigen Adsorption under Shear Oscillation on a Quartz Crystal Microbalance, *Langmuir 194*, 729−734. (b) Hook, F., Rodahl, M., Brezinski, P., Kasemo, B. (1998) Measurements Using the Quartz Crystal Microbalance Technique of Ferritin Monolayers on Methyl-Thiolated Gold: Dependence of Energy Dissipation and Saturation Coverage on Salt Concentration, *J. Colloid Inter. Sci. 208*, 63−67.
19. Yang, M., Thompson, M., Duncan-Hewitt, W. C. (1993) Interfacial Properties and the Response of the Thickness-Shear-Mode Acoustic Wave Sensor in Liquids, *Langmuir 9*, 802−811.
20. (a) Yang, M., Thompson, M. (1993) Surface Morphology and the Response of the Thickness-Shear Mode Acoustic Wave Sensor in Liquids, *Langmuir 9*, 1990−1994. (b) Urbakh, M., Daikhin, L. (1994) Influence of the Surface Morphology on the Quartz Crystal Microbalance Response in a Fluid, *Langmuir 10*, 2836−2841.
21. Cowart, M., Gibson, K. J., Allen, D. J., and Benkovic, S. J. (1998) DNA substrate structural requirements for the exonuclease and polymerase activities of prokaryotic and phage DNA polymerases, *Biochemistry 28*, 1975−1983.

BI048486+